

COMPARATIVE STUDY OF IC, P&O AND FLC METHOD OF MPPT ALGORITHM FOR GRID CONNECTED PV MODULE

¹ M. LAMNADI, ¹M. TRIHI, ²Badre BOSSOUFI, ¹A. BOULEZHAR

¹Department of Physics, Theoretical and Applied Physics Laboratory, University Hassan II Ain Cock
Faculty of Sciences, Casablanca, Morocco

² Laboratory of Electrical Engineering and Maintenance LGEM, Higher School of Technology, EST-
Oujda, University of Mohammed I, Morocco

E-mail: ¹ mouna.lamnadi@gmail.com,

ABSTRACT

The photovoltaic (PV) system is one of the renewable energies that attract the attention of researchers in the recent decades. The PV generators exhibit nonlinear I-V and P-V characteristics. The maximum power produced varies with both irradiance and temperature.

Since the conversion efficiency of PV arrays is very low, it requires maximum power point tracking (MPPT) control techniques. The purpose of this paper is to study and compare three maximum power point tracking (MPPT) methods in a photovoltaic simulation system using perturb and observe method, Incremental conductance method and Fuzzy Logic Control method. MATLAB/Simulink used to establish an Implementation of MPPT Algorithm for Grid Connected PV module.

This system is developed by combining the models established of solar PV module & MPPT, DC-DC Boost converter, DC/AC converter. The system is simulated under different irradiation (between 250 W/m² and 1000 W/m²). Simulation results show that the photovoltaic simulation system can track the maximum power point accurately.

Keywords: *Photovoltaic System, MPPT, Incremental Conductance Method, Perturb And Observe Method, Fuzzy Logic Control Method (FLC) And Simulation Results*

1. INTRODUCTION

World energy consumption is growing every day, and natural resources are limited. Nowadays most of the consumed energy is obtained from fossil fuels, causing environment pollution. If it does not change soon, we will run out of energy sources and there will be energy shortage. Therefore, we need sustainable energy sources, such as solar, wind, hydro, geothermal or biomass.

Solar photovoltaic power generation has a very powerful potential, because of the absence of fuel cost, the scalability in power and the simplicity and little maintenance required by PV systems [1]. More than 45% of necessary energy in the world will be generated by PV arrays [2]. Unfortunately, PV generation systems have two major problems: the conversion efficiency of electric power generation is low, and the amount of electric power generated by solar arrays changes continuously with weather conditions [3]. Moreover, because of nonlinear I-V and P-V characteristics of PV systems, their output power is always changing

with weather conditions, i.e., solar radiation, atmospheric temperature and also nature of load connected [4]. Maximum power point tracking (MPPT) is essential as there is a probable mismatch between the load characteristics and the maximum power points (MPPs) of the PV module in order to ensure optimal utilization of solar cells [5].

Over the years, many MPPT techniques have been advocated, developed and implemented. These methods vary in several aspects such as complexity required number of sensors, convergence speed, cost, range of effectiveness, ease of hardware implementation etc [6].

There are around 20 MPPT techniques that have been developed in the last two decades. Some of these methods/techniques are [7]:

- Hill climbing
- Perturb and observe (P&O)
- Incremental conductance (IncCond)
- Fractional open circuit voltage (Voc)
- Fractional short circuit current (Isc)
- Ripple correlation control (RCC)

- Current sweep
- Fuzzy logic control (FLC)
- Load current or load voltage maximization
- DC link capacitor droop control etc.

2. GLOBAL SOLAR RADIATION

The estimation of global solar radiation is essential for utilization the solar energy, design wherever appropriate observations missing [8]. The values of solar radiation in clear skies are useful for determining the maximum performance heating and photovoltaic as well as for the design of air conditioning equipment in buildings or for the determination of thermal load their solar installations [9].

Sizing and optimal management of energy systems can only be achieved by knowing the weather conditions that extensive studies are carried out in several parts of the world to assess and model the solar potential [10].

The Solar radiation who reaches the ground is formed by a direct radiation and a diffuse radiation which they are together form the global radiation [11-12], we dedicate these respectful radiation respectively by the letters I (direct), D (diffuse) et G (global), all these are calculated with W/m².

2.1 Solar radiation on a horizontal surface full south

2.1.1 Direct solar flux

It can be calculated by the formula:

$$I_h = I_0 * \Gamma * C_t * \exp\left(-\frac{0.13}{\sin(h)}\right) * \sin(h) \quad (1)$$

I_0 (W/m²) is the solar constant, which is defined as the energy flux received by a unit area, in our case, the value that was selected 1367 W/m [13-14], Γ (dimensionless) is the turbidity atmospheric factor for clear skies [15-16], Can be calculated by the formula:

$$\Gamma = 0.796 - 0.01 * \sin[0.986 * (j + 284)] \quad (2)$$

C_t (Dimensionless) is the correction of the earth-sun distance can be calculated by the equation [17]:

$$C_t = 1 + 0.034 * \cos(j - 2) \quad (3)$$

h (Degrees) is the height of the sun, can be calculated by the following formula [18-19]:

$$h = \sin^{-1}(\sin(\varphi) * \sin(\delta) + \cos(\varphi) * \cos(\delta) * \cos(\omega)) \quad (4)$$

δ (degrees) is the solar declination can be calculated by the approximate formula given by Cooper (1969) [18]:

$$\delta = 23.45 * \sin(0.0986 * (j + 284)) \quad (5)$$

Where j is the day number of the year, ranging from 1 on 1 January to 365 on 31 December. (degrees) is the latitude.

(degrees) is the hour angle of the sun, can be calculated by the following equation [18-19]:

$$\omega = 15 * (12 - T_{sv}) \quad (6)$$

T_{sv} (hours) is the true solar time of the study site, it is determined by the formula [20]:

$$T_{sv} = T_l - DT_l + (D_{hg} + E/60)/60 \quad (7)$$

T_l : Local time.

DT_l : Advance the local time through standard time.

D_{hg} : The time difference (advance of 4 min per degree).

E : Equation of time, which is calculated by the equation [21]:

$$E = 450.8 * \sin\left(\frac{2*\pi*j}{365} - 0.026903\right) + 595.4 \sin\left(\frac{2*\pi*j}{365} + 0.352835\right) \quad (8)$$

This formula gives time in seconds

2.1.2 Diffuse solar flux

It can be calculated by the formula:

$$D_h = 120 * \Gamma * \exp\left(-\frac{1}{(0.4511 + \sin(h))}\right) \quad (9)$$

2.1.3 Global solar flux

It is the sum of the direct and diffuse solar radiation [22-23]:

$$G_h = I_h + D_h \quad (10)$$

3. PV SYSTEM MODELING

The solar PV generation system consists of a PV module, the DC/DC boost converter, the VSC converter and the three phase transformer as shown in Fig. 1. Radiation (R) is incident on the PV module. It generates a voltage (V) and current (I) which will be fed into the utility grid.

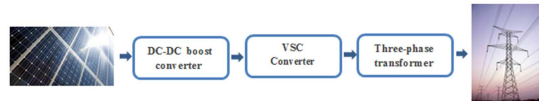


Figure 1: Block Diagram Of Grid-Connected Photovoltaic Power System

3.1 PV solar module

The PV module used in this study consists of 96 polycrystalline silicon solar cells electrically configured as five series strings of 66 cells each. Its main electrical specifications are shown in table 1. The equivalent circuit model for a PV module is addressed in [24-25-26]

The 100-kW PV array of the detailed model uses 330 SunPower modules (SPR-305). The array consists of 66 strings of 5 series-connected modules connected in parallel (66*5*305.2 W= 100.7 kW).

Table 1: The electrical Characteristic of SunPower SPR-305-WHT PV module.

Maximum power (Pmax)	305 W
Voltage at Pmax (Vmp)	54.7 V
Current at Pmax (Imp)	5.58 A
Short-circuit current (Isc)	5.96 A
Open-circuit voltage (Voc)	64.2 V

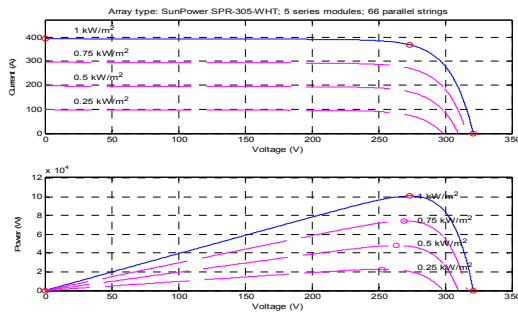


Figure 2: I-V and P-V characteristics of Array at 25°C

3.2 Boost converter DC/DC

According to maximum power transfer theory, maximum power is being transferred from source to load when source impedance is equal to the load impedance (load matching). The load matching can be done by adjusting the duty cycle of the DC/DC converter. The duty cycle is the ratio between the switching on time of switch to the switching period. In order to track MPP the converter must be operated with duty cycle corresponding to it. With varying atmospheric conditions the duty cycle of the DC/DC converter has to be adjusted to extract maximum power from PV module [27]. There are several architectures of DC/DC conversion circuits which can be used for this purpose.

In the present work the boost configuration is chosen due to its wide spread use and high reliability with respect to other more complex configurations [28]. The complete power device scheme is shown in Fig. 3. The diode D is provided to protect the PV module against negative current which could damage it. C placed at boost input to limit the high frequency harmonic components [28].

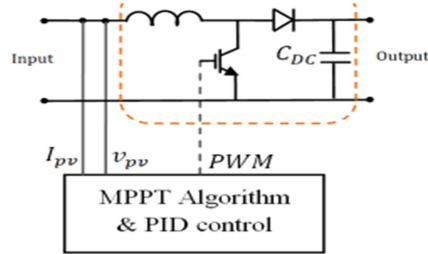


Figure 3: Boost Converter Modeling

4. MPPT TECHNIQUES

In this work, three MPPT techniques have been selected for the purpose of comparison:

Incremental conductance (INC), perturb and observe (P&O) and fuzzy logic controller (FLC).

4.1 Incremental conductance (IC) technique

Among all the MPPT strategies, the incremental conductance technique is widely used due to the high tracking accuracy at steady state and good adaptability to the rapidly changing atmospheric conditions [4]. This technique employs the slope of the PV array power characteristics to track MPP. The slope of the PV array power curve is zero at the MPP, positive for values of output voltage smaller than the voltage at MPP, and negative for values of the output voltage greater than the voltage at MPP. The derivative of the PV module power is given as in (11), and the resultant equation for the error e is as in (12) [29-30-31].

$$\frac{dP}{dV} = \frac{d(V*I)}{dV} = I + V \frac{dI}{dV} = 0 \quad (11)$$

$$\text{Also, } \frac{dI}{dV} + \frac{I}{V} = \frac{I(i)-I(i-1)}{V(i)-V(i-1)} + \frac{I(i)}{V(i)} = 0$$

$$e = \frac{I(i)-I(i-1)}{V(i)-V(i-1)} + \frac{I(i)}{V(i)} \quad (12)$$

Therefore tracking the MPP requires the following procedure as shown in Fig. 4. It can be implemented by a simple discrete integrator with the error signal e as the input, and a scaling factor k. The function of the scaling factor k is to adapt the error signal e to a proper range before the integral compensator. As the operating point approaches the MPP, the error signal e becomes smaller, resulting in an adaptive and smooth tracking [29].

To improve, both, the MPPT speed and accuracy simultaneously a modified dynamic change in step size for INC is introduced [4]. This technique

improves the performance of INC technique but at a cost of increased complexity of the control system.

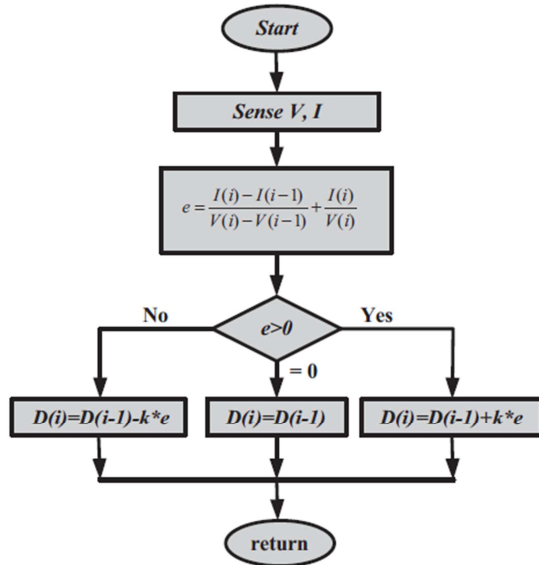


Figure 4: State-flow chart of INC MPPT technique

4.2 Perturb and observe (P&O) technique

P&O is the most frequently used technique to track the maximum power due to its simple structure [32]. This technique operates by periodically perturbing the PV module terminal voltage and comparing the PV output power with that of the previous perturbation cycle [2]. As shown in Fig. 5 if the PV module operating voltage changes and power increases the control system moves the operating point in that direction; otherwise the operating point is moved in the opposite direction.

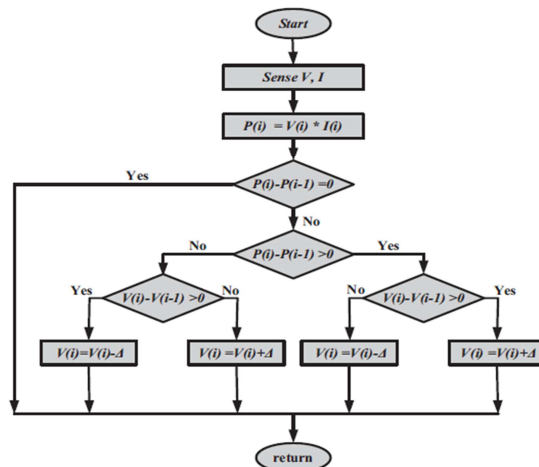


Figure 5: State-flow chart of P&O MPPT technique

4.3 Fuzzy logic controller (FLC) technique

FLC has been introduced in many researches as in [33-34-35-36] to force the PV to work around MPP. FLCs have the advantages of working with imprecise inputs, not needing an accurate mathematical model, and handling nonlinearity. The details of using FLC in MPPT of PV system are shown in [37-38-39]. The error signal can be calculated as shown in (13). The value of DE is calculated as shown in (14).

$$E(k) = \frac{P_{pv}(k) - P_{pv}(k-1)}{V_{pv}(k) - V_{pv}(k-1)} \tag{13}$$

$$dE(k) = E(k) - E(k - 1) \tag{14}$$

Where: $P_{pv}(k)$ and $V_{pv}(k)$ are respectively the instantaneous output powers and output voltage of the photovoltaic generator.

The input $E(k)$ shows if the load operation point at the instant k is located on the left or on the right of the maximum power point on the PV characteristic, while the input $dE(k)$ expresses the moving direction of this point.

The fuzzy inference is carried out by using Madani's method, (Table II), and the defuzzification uses the center of gravity to compute the output of this FLC which is the duty cycle:

$$D = \frac{\sum_{j=1}^n u(D_j)D_j}{\sum_{j=1}^n u(D_j)} \tag{15}$$

The control rules are indicated in Table II with e and dE as Inputs and D as the output.

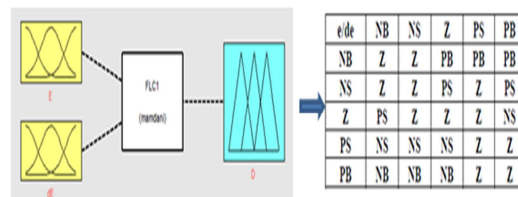


Figure 6: Structure of fuzzy controller

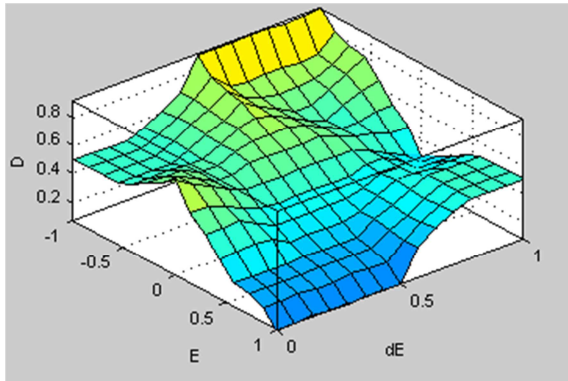


Figure 7: Presentation of 3D (error E, error variation dE and duty cycle D)

5. SIMULATION AND RESULTS

The simulation uses 100-kW PV array is connected to a 25-kV grid via a DC/DC boost converter and a three-phase three-level Voltage Source Converter (VSC). Maximum Power Point Tracking (MPPT) is implemented in the boost converter by means of a Simulink model using three different techniques. The average model contains the following components:

- PV array delivering a maximum of 100 kW at 1000 W/m² sun irradiance (Fig. 10).
- DC-DC boost converter
- 3-level 3-phase VSC
- 100-kVA 260V/25kV three-phase coupling transformer
- Utility grid (25-kV distribution feeder + 120 kV equivalent transmission systems).

The Boost converter DC-DC has a frequency of 5-kHz with increasing voltage from PV natural

voltage (273 V DC at maximum power) to 500 V DC. Switching duty cycle is optimized by a MPPT controller that uses three techniques. This MPPT system automatically varies the duty cycle in order to generate the required voltage to extract maximum power.

The VSC converts the 500V DC link voltage to 260V AC and keep unity power factor. The VSC control system uses two control loops:

- External control loop which regulates DC link voltage to +/- 250 V ;
- Internal control loop which regulates Id and Iq grid currents (active and reactive current components).

Id current reference is the output of the DC voltage external controller. Iq current reference is set to zero in order to maintain unity power factor. Vd and Vq voltage outputs of the current controller are converted to three modulating signals Uabc_ref used by the PWM Generator. The control system uses a sample time of 100 microseconds for voltage and current controllers as well as for the PLL synchronization unit. Pulse generators of Boost and VSC converters use a fast sample time of 1 microsecond in order to get an appropriate resolution of PWM waveforms. PV array used in simulation delivers a maximum of 300 kW at 1000 W/m² irradiance. VSC produces harmonics which is filtered by a 10-kvar capacitor bank, Three-phase coupling transformer has a rating of 100-kVA 260V/25KV .Utility grid has specification of (25-kV distribution feeder + 120 kV equivalent transmission system).

5.1 Simulation of grid connected PV module with IC as MPPT algorithm

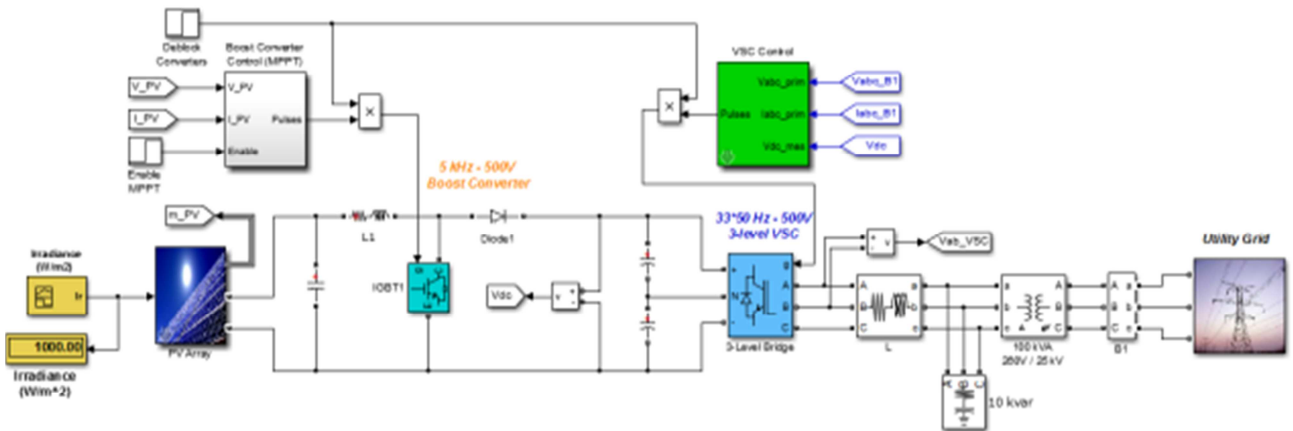


Figure 8: PV Array with MPPT Controllers using "Incremental Conductance" technique for 100-kW Grid-Connected

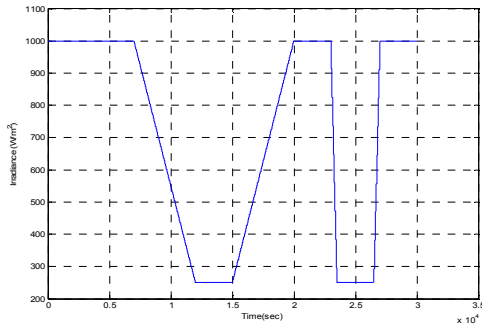


Figure 9: Variation of solar radiation vs time

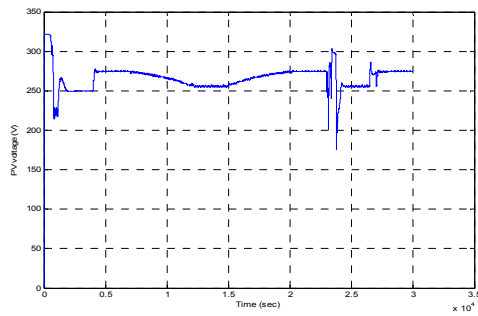


Figure 10: Variation of PV voltage vs time

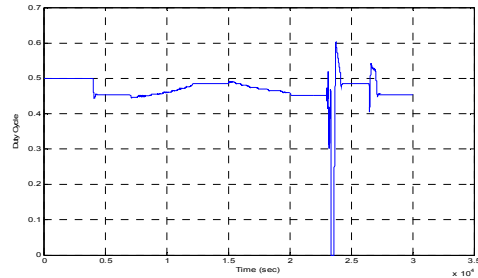


Figure 11: Variation of Duty Cycle vs time

The figures 12-13 are the output at Boost Converter DC/DC

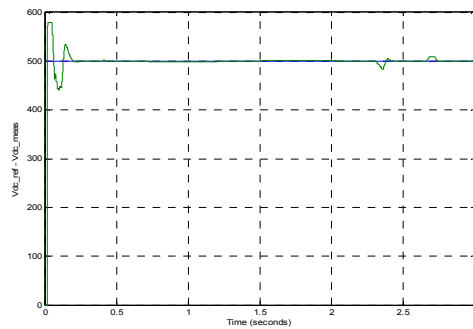


Figure 12: Measured Voltage and Reference Voltage vs time (V_{dc_ref} - V_{dc_meas})

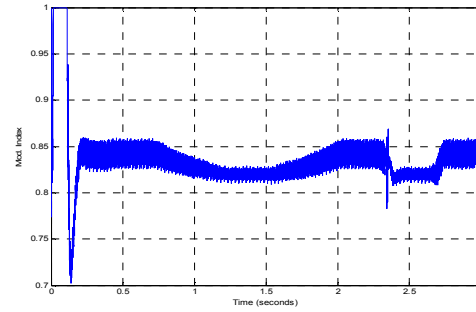


Figure 13: Modulation Index vs time (Mod.Index)

The figure number 14 is the Output of voltage source converter VSC

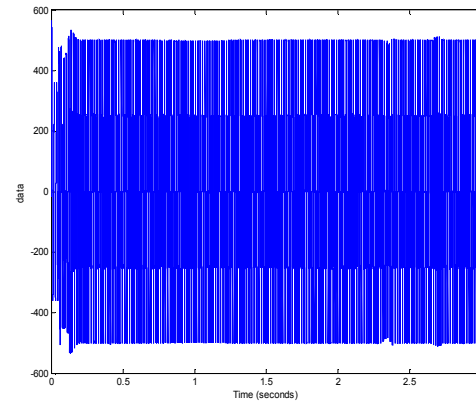


Figure 14: Variation of Output at the inverter V_{ab} vs time

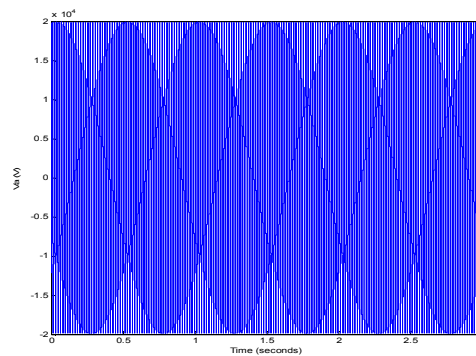


Figure 15: Variation of the Voltage output (V_a) at the utility grid

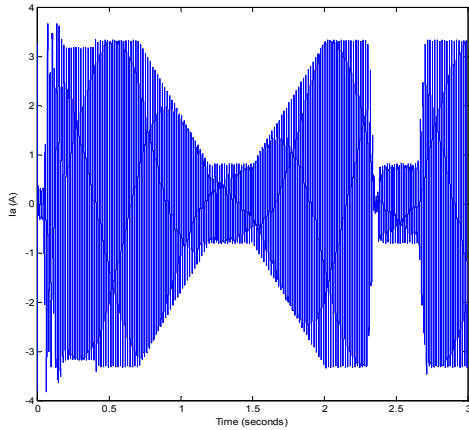


Figure 16: Variation of the current output (I_a) at the utility grid vs time

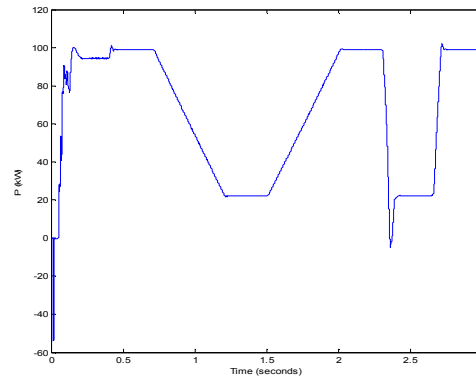


Figure 17: Variation of the power output at the utility grid vs time

5.2 Simulation of grid connected PV module with P&O as MPPT algorithm

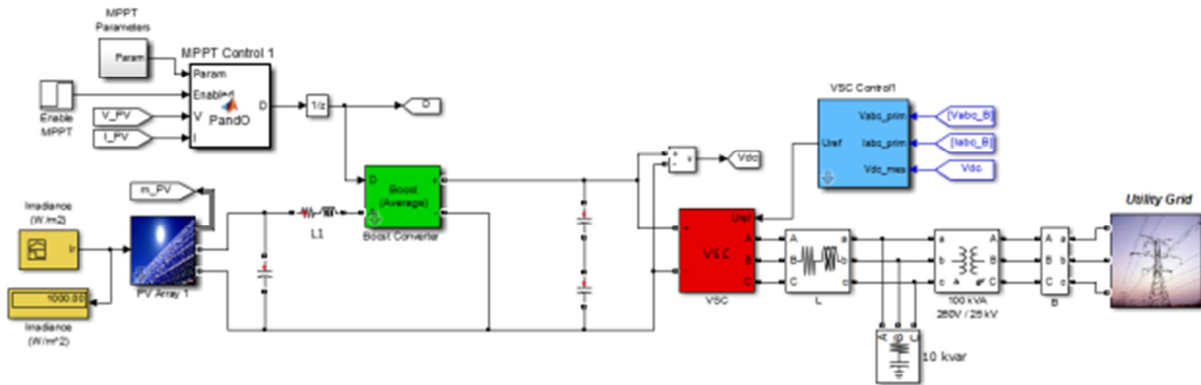


Figure 18: PV Array with MPPT Controllers using "Perturb & Observe" technique for 100-kW Grid-Connected

The main difference between the previous model and this model is in the way that DC-DC boost converter and three phases VSC are modeled. In this model the boost and VSC converters are represented by equivalent voltage sources generating the AC voltage averaged over one cycle of the switching frequency. Such a model does not represent harmonics, but the dynamics resulting from control system and power system interaction is preserved.

This model allows using much larger time steps than the detailed model (50 microseconds v/s 1 microsecond), resulting in a much faster simulation. In the IC model the PV-array model contains an algebraic loop. This algebraic loop is required to get an iterative and accurate solution of the PV model when large sample times are used. This algebraic loop is easily solved by Simulink. The

'Perturb and Observe' MPPT algorithm is implemented in the MPPT Control MATLAB Function block.

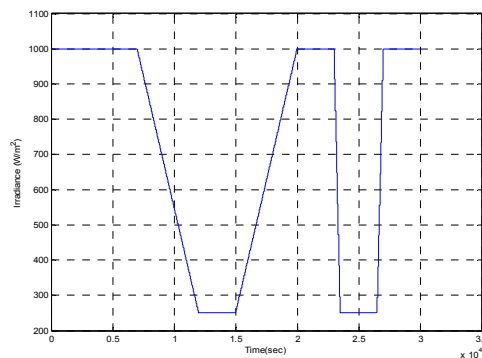


Figure 19: Variation of solar radiation vs time

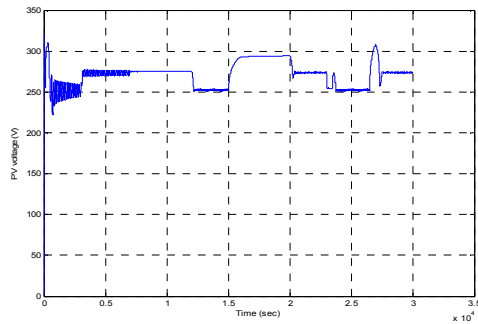


Figure 20: Variation of PV voltage vs time

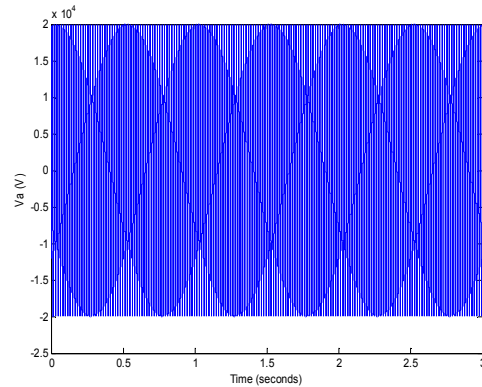


Figure 24: Variation of the Voltage output (V_a) at the utility grid vs time

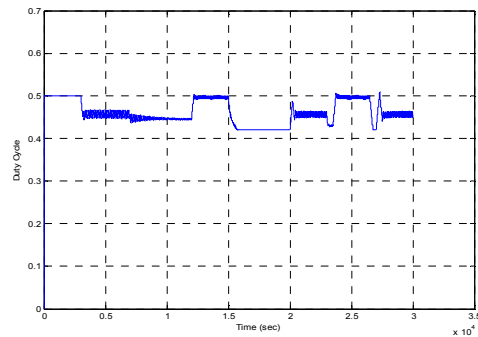


Figure 21: Variation of Duty Cycle vs time

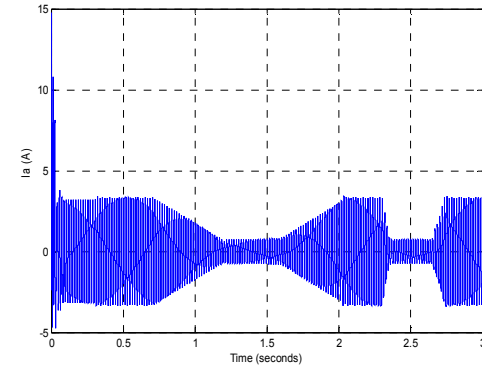


Figure 25: Variation of the current output (I_a) at the utility grid vs time

The figures 22-23 are the output at Boost Converter DC/DC

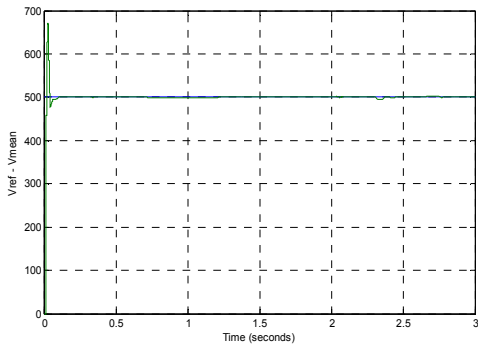


Figure 22: Measured Voltage and Reference Voltage vs time ($V_{dc_ref} - V_{dc_meas}$)

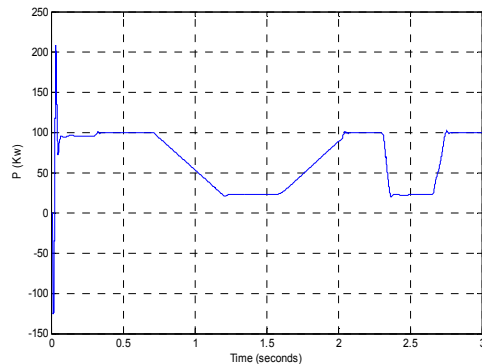


Figure 26: Variation of the power output at the utility grid vs time

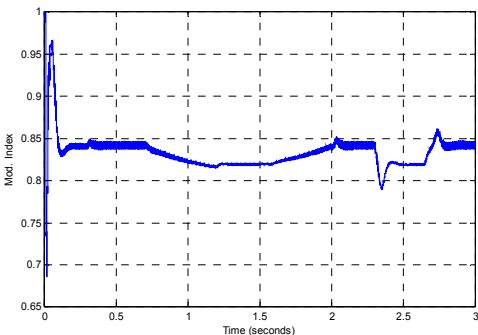


Figure 23: Modulation Index vs time ($Mod.Index$)

5.3 Simulation of grid connected PV module with FLC as MPPT algorithm

This model is the same one used when we simulated P&O as MPPT algorithm

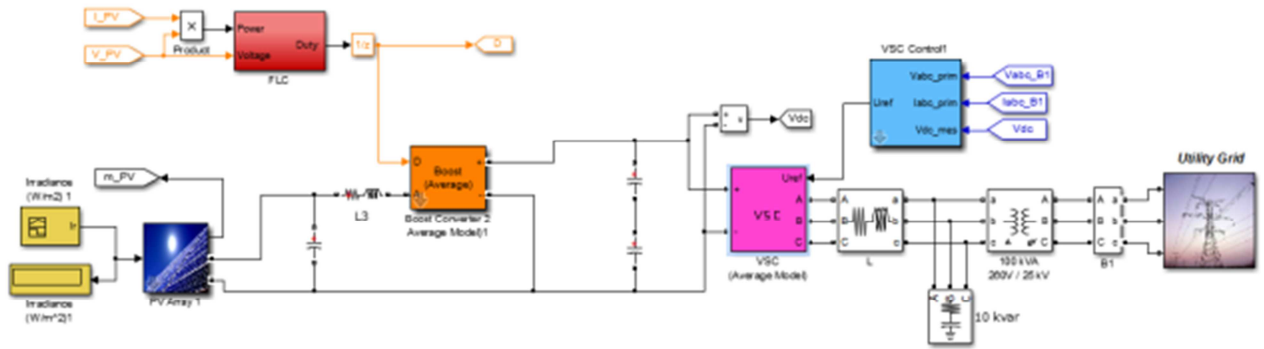


Figure 27: PV Array with MPPT Controllers using "FLC" technique for 100-kW Grid-Connected

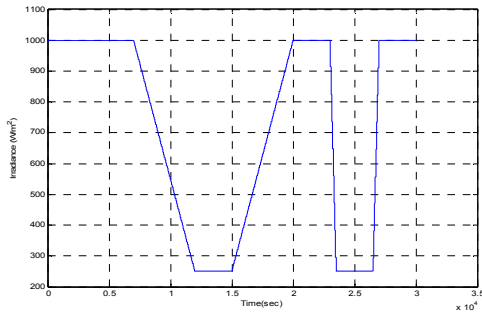


Figure 28: Variation of solar radiation vs time

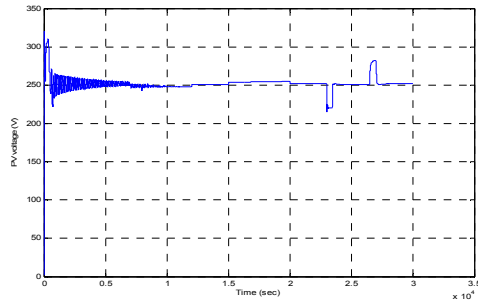


Figure 29: Variation of PV voltage vs time

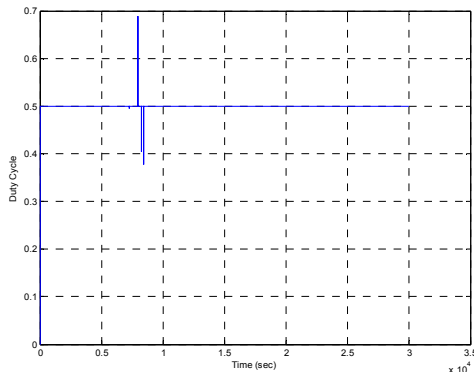


Figure 30: Variation of Duty Cycle vs time

The figures 31-32 are the output at Boost Converter DC/DC

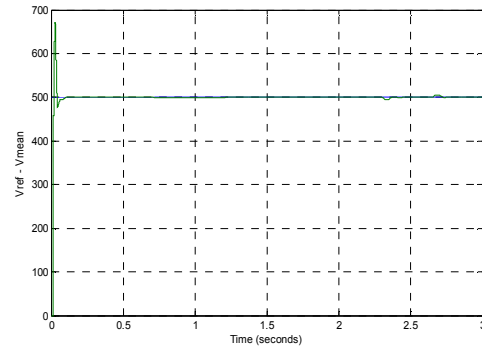


Figure 31: Measured Voltage and Reference Voltage vs time ($V_{dc_ref} - V_{dc_meas}$)

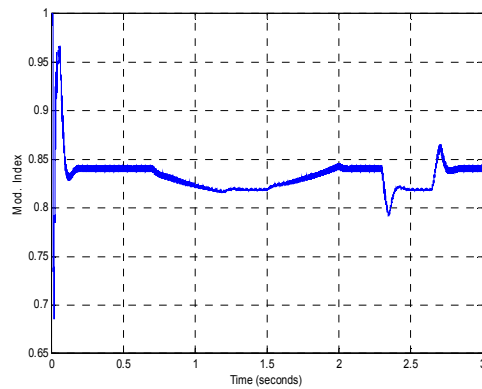


Figure 32: Modulation Index vs time (Mod.Index)

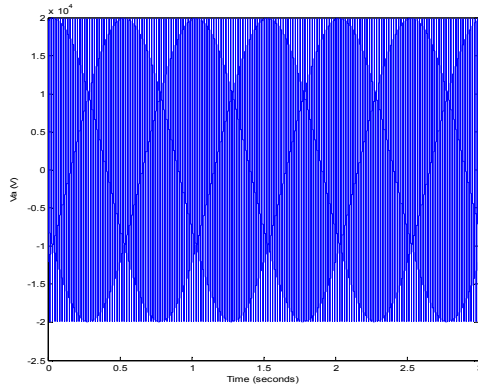


Figure 33: Variation of the Voltage output (V_a) at the utility grid vs time

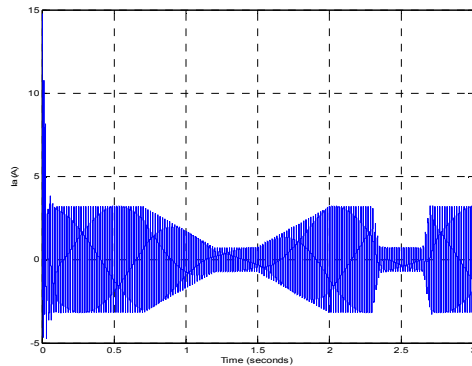


Figure 34: Variation of the current output (I_a) at the utility grid vs time

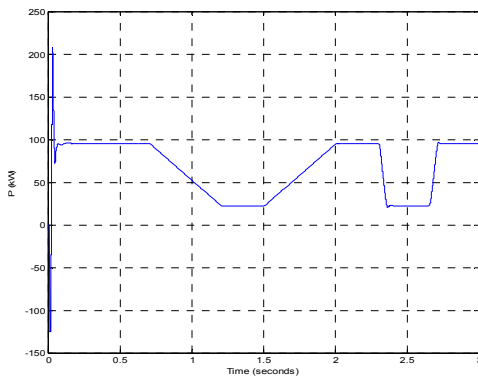


Figure 35: Variation of the power output at the utility grid vs time

4. COMPARATIVE STUDY OF RESULTS

A comparative study is performed with IC, P&O and FLC MPPT methods. The comparisons shows that with same varying irradiance values the area under the curve in power plot is more in FLC than P&O and IC algorithm but more power is generated

using IC algorithm than P&O and FLC algorithm with same varying irradiance values.

In IC Voltage curve settle down fast than P&O and FLC. So IC algorithm leads to less settling time.

This study prove that the perturb-and-observe, incremental conductance and Fuzzy Logic Control methods should have very similar overall efficiencies, but that incremental conductance should be slightly better ($P=99.04$ Kw).

However, the results of this study indicate that, to within the accuracy available, the MPPT efficiencies of the incremental conductance, perturb-and-observe and Fuzzy Logic Control MPPT algorithms are essentially the same.

Furthermore P&O and IC had the same performance under clear sky conditions, indicating that the penalty in efficiency caused by the oscillation about the MPP inherent in P&O under steady-state conditions was insignificant for the optimized algorithms. Incremental conductance Outperformed P&O under partly cloudy conditions, as expected, but the difference was very small.

Also, interestingly, FLC had a significantly higher efficiency than incremental conductance under cloudy skies.

Simulation works confirm the best performance of Fuzzy Logic Control MPPT algorithm to achieve low oscillation and overshoot, which contributes to high stability operation.

5. CONCLUSION

A Photovoltaic system not only consist of PV modules but also involves good deal of power electronics as an interface between PV modules and load for effective and efficient utilization of naturally available Sun power. Such a PV model is easy to be used for the implementation on MATLAB/Simulink modeling and simulation platform.

Simulation of PV module and MPPT to maximize power has been performed. the different MPPT methods used in this paper are Perturb and Observe method, Incremental Conductance method and Fuzzy Logic Controller method.

The proposed algorithms has been demonstrated, also comparative evaluation was carried them to obtain results which verify their performance.

REFERENCES:

- [1] Á.-A. Bayod-Rújula and J.-A. Cebollero-Abián, "A novel MPPT method for PV systems with irradiance measurement", *Solar Energy*, vol. 109, p. 95–104, 2014.

- [2] R. Faranda, S. Leva, et V. Maugeri, "MPPT techniques for PV systems: energetic and cost comparison", in *Power and Energy Society General Meeting-Conversion and Delivery of Electrical Energy in the 21st Century, 2008 IEEE, 2008*, p. 1–6.
- [3] M. Berrera, A. Dolara, R. Faranda, et S. Leva, "Experimental test of seven widely-adopted MPPT algorithms", in *PowerTech, 2009 IEEE Bucharest, 2009*, p. 1–8.
- [4] F. Liu, S. Duan, F. Liu, B. Liu, and Y. Kang, "A variable step size INC MPPT method for PV systems", *Industrial Electronics, IEEE Transactions on*, vol. 55, no 7, p. 2622–2628, 2008.
- [5] W. Xiao and W. G. Dunford, "A modified adaptive hill climbing MPPT method for photovoltaic power systems", in *Power Electronics Specialists Conference, 2004. PESC 04. 2004 IEEE 35th Annual, 2004*, vol. 3, p. 1957–1963.
- [6] J. C. Schaefer, "Review of photovoltaic power plant performance and economics", *IEEE Transactions on Energy Conversion (Institute of Electrical and Electronics Engineers);(USA)*, vol. 5, no 2, 1990.
- [7] S. Leva, D. Zaninelli, and R. Contino, "Integrated renewable sources for supplying remote power systems", *WSEAS transactions on power systems*, vol. 2, no 2, p. 41, 2007.
- [8] T. Konzelmann, R. S. van de Wal, W. Greuell, R. Bintanja, E. A. Henneken, et A. Abe-Ouchi, "Parameterization of global and longwave incoming radiation for the Greenland Ice Sheet", *Global and Planetary change*, vol. 9, no 1, p. 143–164, 1994.
- [9] A. C. de la Casinière, "Le rayonnement solaire dans l'environnement terrestre", *Editions Publibook, 2003*.
- [10] Bekkouche, S.M.A, "Modélisation du Comportement Thermique de Quelques Dispositifs Solaires", *Thèse de Doctorat, Option Electronique et Modélisation, L'université Abou-Bakr Belkaïd – Tlemcen, 2008–2009*
- [11] Bertrand, A., "Exploitation Des Nouvelles Capacités D'observation De La Terre Pour Evaluer Le Rayonnement Solaire Incident Au Sol", *Thèse de Doctorat, ED N 432: Science des Métiers de l'Ingénieur, école nationale supérieure des mines de Paris. 1980*
- [12] R. Bernard, G. Menguy, et M. Schwartz, "Le rayonnement solaire, Conversion thermique et applications", 1979.
- [13] M. Fekih, M. Saighi, et C. D. R. S. P. "Les Régions Humide", *Semi-Aride Et Aride De l'Algérie. application a l'évaporation des barrages*, vol. 6.
- [14] L. T. Wong et W. K. Chow, "Solar radiation model", *Applied Energy*, vol. 69, no 3, p. 191–224, 2001.
- [15] M. Capderou, Atlas Solaire de l'Algérie, "Modèles Théoriques et Expérimentaux", *Office des Publications Universitaires, Algérie, 1987*.
- [16] Y. Bouhadda et L. Serrir, "Contribution à l'étude du trouble atmosphérique de Linke sur le site de Ghardaïa", *Revue des énergies renouvelables*, vol. 9, no 4, p. 277–284, 2006
- [17] C. Vauge, C. P. de Brichambaut, C. P. de Brichambaut, F. Meteorologist, C. P. de Brichambaut, et F. Météorologue, "Le gisement solaire: Evaluation de la ressource énergétique. Technique et documentation-Lavoisier", 1982.
- [18] K. Danel et L. Gautret, "Génération du disque solaire des communes de l'Ouest", *ARER, Mars-Août, 2008*.
- [19] M. HAMDANI, "Étude et Effet de l'Orientation de deux Pièces d'un Habitat en Pierre Situé à Ghardaïa", 2011.
- [20] M. Nia, M. Chegaar, M. F. Benatallah, et M. Aillerie, "Contribution to the quantification of solar radiation in Algeria", *Energy Procedia*, vol. 36, p. 730–737, 2013.
- [21] A. M'Rouï, S. Mouhous, A. Malek, et B. Benyoucef, "Etude statistique du rayonnement solaire à Alger", *Revue des Energies Renouvelables*, vol. 14, no 4, p. 637–648, 2011.
- [22] M. R. Yaïche et S. M. A. Bekkouche, "Conception et Validation d'un Programme Sous Excel pour l'Estimation du Rayonnement Solaire Incident en Algérie. Cas d'un Ciel Totalelement Clair", *Revue des Energies Renouvelables*, vol. 11, no 3, p. 423–436, 2008.
- [23] M. Mesri-Merad, I. Rougab, A. Cheknane, and N. I. Bachari, "Estimation du rayonnement solaire au sol par des modèles semi-empiriques", *Revue des Energies Renouvelables*, vol. 15, no 3, p. 451–463, 2012.
- [24] G. A. Jebaselvi and S. Paramasivam, "Analysis on renewable energy systems", *Renewable and Sustainable Energy Reviews*, vol. 28, p. 625–634, 2013.
- [25] N. Khaehintung, T. Wiangtong, and P. Sirisuk, "FPGA implementation of MPPT using variable step-size P&O algorithm for PV applications", in *Communications and*



- Information Technologies, 2006. ISCIT'06. International Symposium on, 2006, p. 212–215.*
- [26] J. C. M. Raj and A. E. Jeyakumar, “A two stage successive estimation based maximum power point tracking technique for photovoltaic modules”, *Solar Energy, vol. 103, p. 43–61, 2014.*
- [27] A. R. Reisi, M. H. Moradi, and S. Jamasb, “Classification and comparison of maximum power point tracking techniques for photovoltaic system: a review”, *Renewable and Sustainable Energy Reviews, vol. 19, p. 433–443, 2013.*
- [28] M. Berrera, A. Dolara, R. Faranda, and S. Leva, “Experimental test of seven widely-adopted MPPT algorithms”, in *PowerTech, 2009 IEEE Bucharest, 2009, p. 1–8.*
- [29] H. Abouobaida and M. Cherkaoui, “Comparative study of maximum power point trackers for fast changing environmental conditions”, in *Multimedia Computing and Systems (ICMCS), 2012 International Conference on, 2012, p. 1131–1136.*
- [30] Y.-T. Chen, Z.-H. Lai, and R.-H. Liang, “A novel auto-scaling variable step-size MPPT method for a PV system”, *Solar Energy, vol. 102, p. 247–256, 2014.*
- [31] H. Rezk and A. M. Eltamaly, “A comprehensive comparison of different MPPT techniques for photovoltaic systems”, *Solar Energy, vol. 112, p. 1–11, 2015.*
- [32] I. V. Banu, R. Beniuga, and M. Istrate, “Comparative analysis of the perturb-and-observe and incremental conductance MPPT methods”, in *Advanced Topics in Electrical Engineering (ATEE), 2013 8th International Symposium on, 2013, p. 1–4.*
- [33] D. S. Karanjkar, S. Chatterji, A. Kumar, et S. L. Shimi, “Fuzzy adaptive proportional-integral-derivative controller with dynamic set-point adjustment for maximum power point tracking in solar photovoltaic system”, *Systems Science & Control Engineering: An Open Access Journal, vol. 2, no 1, p. 562–582, 2014.*
- [34] M. Azzouzi, “Comparaison between MPPT P&O and MPPT fuzzy controls in optimizing the photovoltaic generator”, *International Journal of Advanced Computer Science and Applications, vol. 3, no 12, 2012.*
- [35] C. B. Salah, M. Chaabene, and M. B. Ammar, “Multi-criteria fuzzy algorithm for energy management of a domestic photovoltaic panel”, *Renewable Energy, vol. 33, no 5, p. 993–1001, 2008.*
- [36] R. Rajesh and M. C. Mabel, “Efficiency analysis of a multi-fuzzy logic controller for the determination of operating points in a PV system”, *Solar Energy, vol. 99, p. 77–87, 2014.*
- [37] A. M. Eltamaly, A. I. Alolah, et M. Y. Abdulghany, “Digital implementation of general purpose fuzzy logic controller for photovoltaic maximum power point tracker”, in *Power Electronics Electrical Drives Automation and Motion (SPEEDAM), 2010 International Symposium on, 2010, p. 622–627.*
- [38] A. M. Eltamaly, “Modeling of fuzzy logic controller for photovoltaic maximum power point tracker”, in *Solar Future 2010 Conference, Istanbul, Turkey, 2010.*
- [39] G. A. Jebaselvi and S. Paramasivam, “Analysis on renewable energy systems”, *Renewable and Sustainable Energy Reviews, vol. 28, p. 625–634, 2013.*